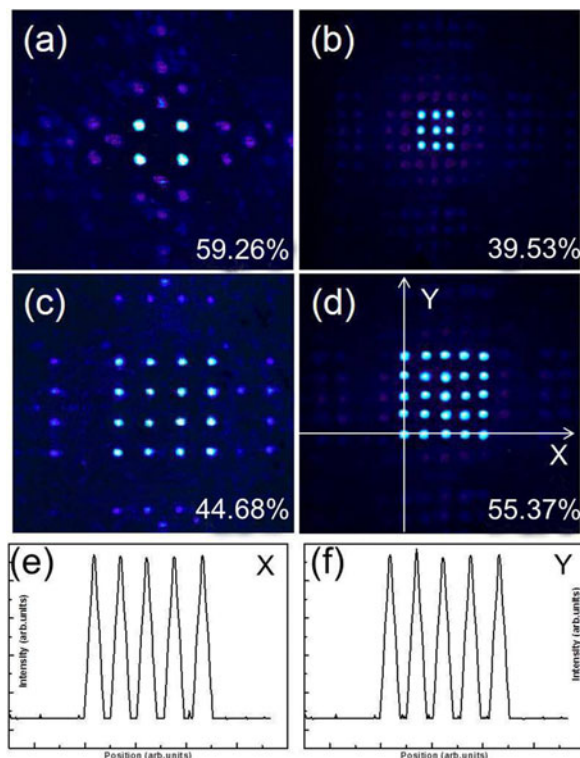


Sapphire-Based Dammann Gratings for UV Beam Splitting

Volume 8, Number 6, December 2016

Qian-Kun Li
Qi-Dai Chen
Li-Gang Niu
Yan-Hao Yu
Lei Wang
Yun-Lu Sun
Hong-Bo Sun, *Member, IEEE*



DOI: 10.1109/JPHOT.2016.2620343

1943-0655 © 2016 IEEE

Sapphire-Based Dammann Gratings for UV Beam Splitting

Qian-Kun Li, Qi-Dai Chen, Li-Gang Niu, Yan-Hao Yu, Lei Wang,
Yun-Lu Sun, and Hong-Bo Sun, *Member, IEEE*

State Key Laboratory on Integrated Optoelectronics, College of Electronic Science and Engineering, Jilin University, Changchun 130012, China

DOI:10.1109/JPHOT.2016.2620343

1943-0655 © 2016 IEEE. IEEE. Translations and content mining are permitted for academic research only. Personal use is also permitted, but republication/redistribution requires IEEE permission. See http://www.ieee.org/publications_standards/publications/rights/index.html for more information.

Manuscript received September 21, 2016; accepted October 18, 2016. Date of publication October 21, 2016; date of current version November 29, 2016. This work was supported by the National Natural Science Foundation of China under Grant 61137001, Grant 61590930, Grant 91323301, Grant 91423102, and Grant 61435005. Corresponding author: Q. D. Chen (email: chenqd@jlu.edu.cn).

Abstract: We report sapphire-based Dammann gratings (DGs) for ultraviolet (UV) beam (266 nm) splitting, which is fabricated via femtosecond laser direct writing assisted with subsequent wet etching. By applying 400-nm-wavelength laser processing followed by wet etching, smooth surface morphology, together with well-tailored geometry, was obtained. These DGs generated 2×2 , 3×3 , 4×4 , and 5×5 spot sources in the fan-out as designed and exhibited diffraction efficiency of 59.26%, 39.53%, 44.68%, and 55.37%, respectively, comparable with theoretical values. Such sapphire-based DGs show great potential in UV beam shaping, UV beam splitting, and laser parallel microprocessing.

Index Terms: Fabrication and characterization, ultraviolet (UV) lasers, micro-optics, laser amplifiers.

1. Introduction

Dammann gratings (DGs), which were invented in the 1970s [1], [2], are considered as a satisfactory class of optical elements that shift a single input light beam into an array of identical outputs. Over the past four decades, attentions have been paid to the design [3]–[6] and fabrication [7]–[9] of this optical device for its wide applications such as beam splitting [10], [11], parallel micro-processing [12], encoding [13], [14], creating 3-D focus spot array and optical vortex rings [15]–[19], multiple imaging [20], and multiplexing technology for practical communication [21], [22]. The above-mentioned works are mostly concentrated for the visible spectral range. Recently, Li *et al.* demonstrated that all-silicon-nanorod-based Dammann gratings could be used for infrared (IR) beam shaping [23]. Although they are also useful for manipulation of ultraviolet (UV) light and UV photo-fabrication, DGs for UV wavelengths are rarely reported to our knowledge. Enabling UV DGs needs appropriate and tractable UV optical materials. As an excellent and frequently-used optical material for Mid-IR-to-UV wavelengths, sapphire is endowed with high thermal and chemical stabilities, hardness, and light transparency. Even though some low-efficiency and high-cost approaches (e. g., electron beam lithography) are applicable, machining difficulty of sapphire still blocks its better utilization for UV micro-optics. Additionally, photolithography and plasma dry etching are also commonly used for patterning sapphire substrate in gallium-nitride-based blue LEDs [24], [25]. However, the

mask-dependent and relatively complicated lithographic process may not simply copy and transfer original pattern of the prototype mask onto the sapphire substrates. In particular, for sapphire, when transferring the cylindrical pillar protrusion polymer mask onto sapphire, conical structures will form on sapphire [24], which is different from the steep transferring on silicon. As a promising solution to above dilemmas, femtosecond laser direct writing (FsLDW) is a maskless, facile, and rapid-writing approach that can “write” out arbitrary, designable and complicated architectures with a nanometric resolution [26]–[28].

In this work, sapphire-based Dammann gratings fabricated by femtosecond laser direct writing assisted with subsequent wet etching for UV beam splitting have been demonstrated. Because laser-sapphire interaction is a coulomb micro-explosion process, femtosecond laser ablation may cause material fracture and, therefore, surface roughness not satisfying the requirements of optical applications. Here, we adopt 400-nm-wavelength laser processing for a higher machining precision and near-threshold processing to solve the material fracture problem, and use wet-etching method to reduce the surface roughness of laser processed areas. Layer-by-layer scanning method was adopted to control the depth of geometrical profile of fabricated DGs on the surface of sapphire. Furthermore, after wet etching, the surface roughness of as formed DGs decreased conspicuously compared with DGs without etching. The as-formed DGs exhibited not only excellent surface quality but also well-defined geometry. Finally, we obtained unique UV beam splitting properties comparable with the theoretical values.

2. Experiments

In our experiment, laser source (Spectra-Physics Solstice) was delivering 120-fs pulses of 800-nm wavelength at repetition rate of 2.5 kHz. We use a BBO crystal to get 400-nm laser light for fabrication, because shorter laser wavelength helps to have a higher machining precision. Pulse energy was measured in front of the objective. Samples of a c-plane sapphire (HEFEI KEJING MATERIALS TECHNOLOGY CO., LTD.) for 3-D laser processing were polished to 430 μm thickness and scanned by tightly focused femtosecond laser pulses through a high numerical aperture ($\text{NA} = 0.85$, 80x) objective lens. To achieve 3-D microstructures, a two-galvano-mirror set was used to control the sample's horizontal scanning. Simultaneously, the beam's vertical movements were performed by a piezo stage with 1 nm precision (PI P-622 ZCD). The complicated 3-D geometry of microstructures was first designed in C# and then converted to computer processing data for 3-D scanning. After femtosecond laser fabrication and wet etching, the as-formed micro-DGs could be obtained on the surface of sapphire. The scanning electron microscopy (SEM) characterization was carried out using a field emission scanning electron microscope (JSM-7500F; JEOL, JEOL Ltd., Tokyo, Japan.), and the samples were sputter-coated with Au film with a thickness of 10 nm (at a current of 20 mA for 60 s) using an auto fine coater (JFC-1600; JEOL). Here, the optical performances of the DGs on sapphire were evaluated by a continuous laser with 266 nm wavelength (Coherent Inc.).

3. Result and Discussions

The laser processing parameters have to be carefully optimized because the excellent geometry quality and surface quality are the prerequisites for the optical properties of DGs on the surface of sapphire. In order to find the optimal processing conditions which play important roles in determining the quality of the 3-D geometry and the quality of the micro structure surface, and, furthermore, the final optical properties of the DGs on sapphire. We first investigated the effects of laser power density, scanning speed and the numerical aperture (NA) of the microscope objective on the characteristics of laser ablation area. The exposure time on a single point was fixed at 1000 μs and the scanning step is 100 nm. When the laser power was 40 μW , close to the threshold of 38 μW , the best surface quality was obtained after wet etching which has been detailed described in our previous work [29]. Four different types of grating structures that generate 2×2 , 3×3 , 4×4 , 5

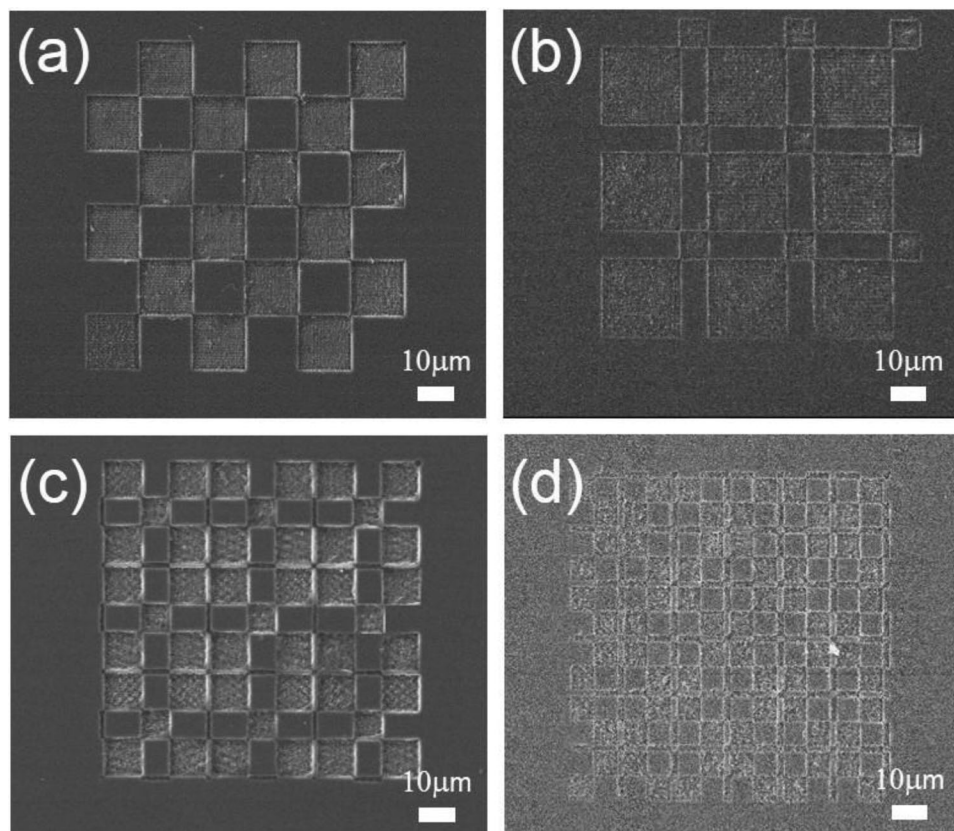


Fig. 1. SEM images of the DGs fabricated by femtosecond laser direct writing without wet etching that generate (a) 2×2 , (b) 3×3 , (c) 4×4 , and (d) 5×5 spot sources, respectively.

$\times 5$ spot sources, respectively, prepared by femtosecond laser direct writing without wet etching are shown in Fig. 1. The data that was adopted in fabricated the Dammann gratings shown in Fig. 1 came from Zhou and Liu [6]. Obviously, a lot of debris generated by femtosecond laser ablation sapphire is on the laser processing area which would deteriorate transmittance of incident light. Then, we adopt wet etching method to remove the debris and periodic nanostructure induced by laser processing.

The top SEM view of DGs, shown in Fig. 2, on the surface of sapphire were fabricated by FsLDW and subsequent wet etching use our optimized best laser processing parameters. Following laser fabrication, the DGs on sapphire were etching 6min in a mixture of sulfuric acid and phosphoric acid (3:1) at 300 centigrade, obviously, the surface roughness got a remarkable change compared with DGs without etching shown in Fig. 1. Actually, the monocrystalline sapphire that interaction with laser transformed to amorphized sapphire which showed extremely high selectivity (calculated) etching with an aqueous solution of a mixture of sulfuric acid and phosphoric acid (3:1). The actual etching rate, measured as the thinning rate of the crystalline sapphire sample in a mixture of sulfuric acid and phosphoric acid (3:1) aqueous solution, was negligible: $< 1 \text{ nm min}^{-1}$. This high selectivity property allows us to freely control depth of fabricated DGs on sapphire. Actually, lots of defects should be located just below the laser ablated and wet-etched surface [30]. High optical performance could be obtained by the method of high temperature ($1100 \text{ }^\circ\text{C}$) annealing to remove the defects.

The depth of the DGs on the surface of sapphire was approximately 162 nm, which was demonstrated by atomic force microscope (AFM), as shown in Fig. 3. The thickness of phase transition

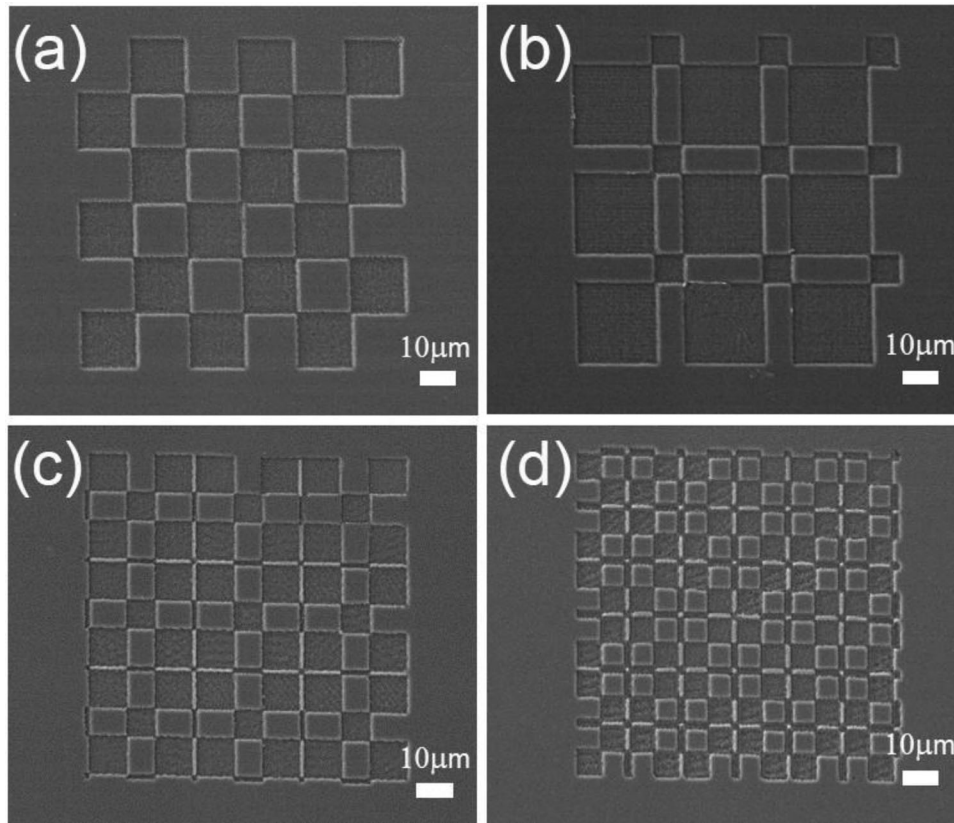


Fig. 2. SEM images of the DGs fabricated by femtosecond laser direct writing with subsequent wet etching that generate (a) 2×2 , (b) 3×3 , (c) 4×4 , and (d) 5×5 spot sources, respectively.

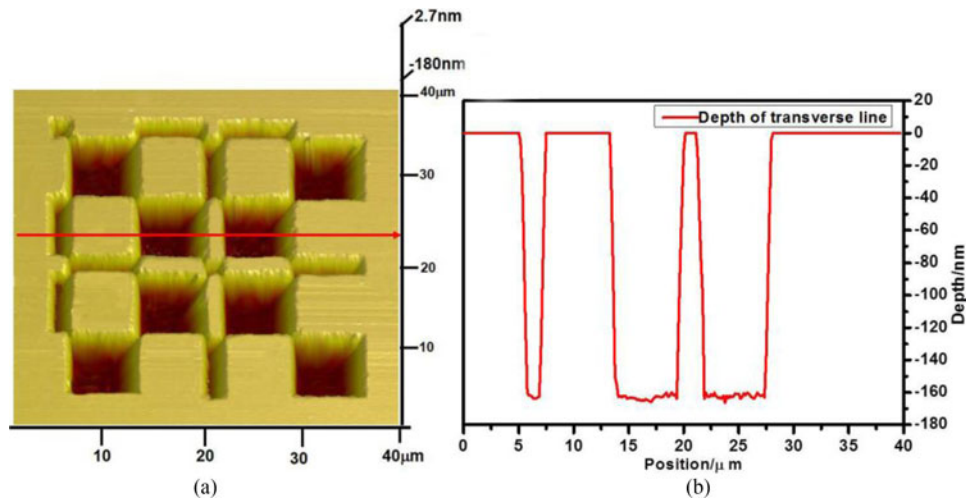


Fig. 3. AFM 3-D image of fabricated DGs on sapphire. (a) AFM characterization exhibiting 3-D morphology of single-period DGs. (b) Cross section at the central line of the single-period DGs by AFM.

areas is associated with several parameters, such as

$$d = \frac{\lambda \varphi}{2\pi \cdot \Delta n}. \quad (1)$$

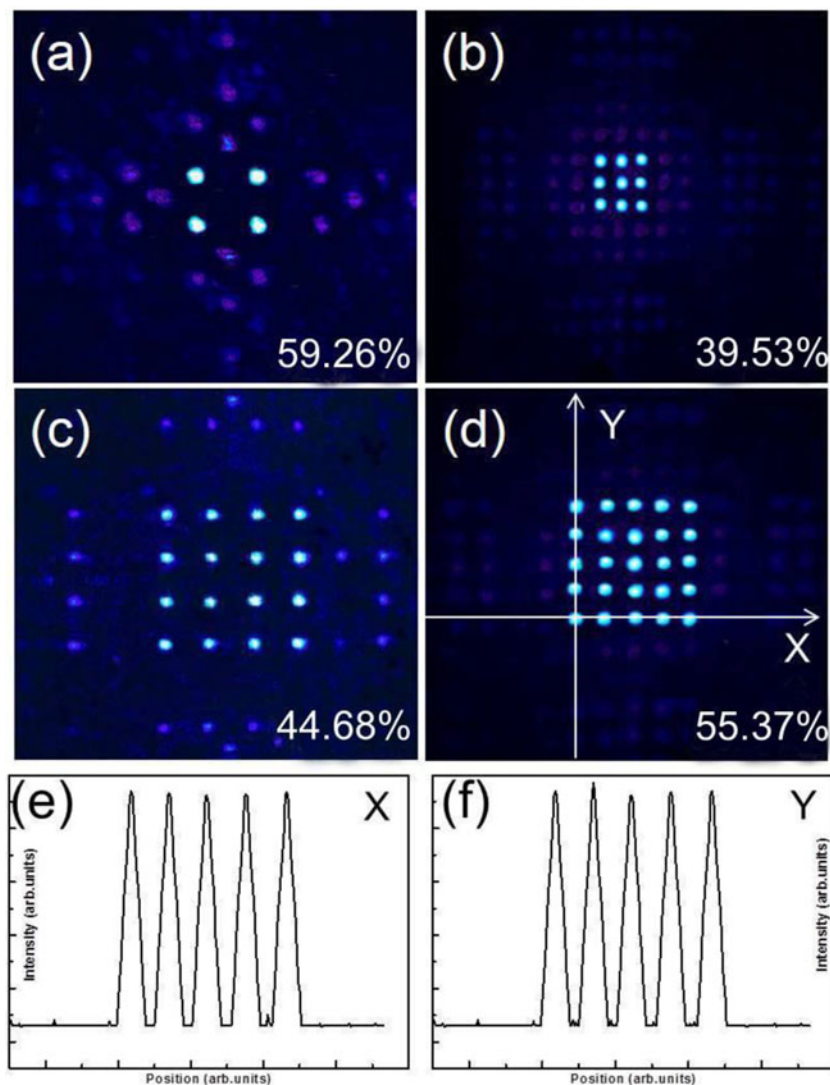


Fig. 4. UV beam splitting performance of the fabricated DGs. The diffraction efficiency of DGs that generate (a) 2×2 , (b) 3×3 , (c) 4×4 , and (d) 5×5 spot sources are 59.26%, 39.53%, 44.68%, and 55.37%, respectively. (e), (f) Intensity distribution of spots along dashed lines X and Y [shown in (d)].

Herein, d is the thickness of phase transition areas; Δn is the difference of the refractive index of sapphire and that of air; φ is the value that phase shifts by; and λ is working wavelength of DGs. The refractive index of sapphire is known to be 1.83 for wavelength 266 nm while that of air is 1.0003. For this type of Dammann grating, in order to ensure the maximum diffractive efficiency, φ should be π . All the DGs we fabricated were supposed to split a continuous laser beam with the wavelength of 266 nm. Therefore, the theoretical thickness for the maximum diffractive efficiency was calculated to be 160.24 nm. The error of the experimental depth with the theoretical depth is less than 5 nm. Here, layer-by-layer scanning method was adopted to control the depth of the DGs. After the upper layer of DGs on sapphire was processed, debris left which will effect further processing. Debris was cleaned by laser (below damage threshold) for further processing. Wet etching also has a certain influence on depth accuracy of DGs. We have done some preliminary compensation corresponding to the error that corrosion may cause when we carry on the theoretical design. Owing to the high refractive index difference between sapphire and air, a grating structure can be much thinner than made in silica glass by photo-induced refractive effect [31]. The femtosecond

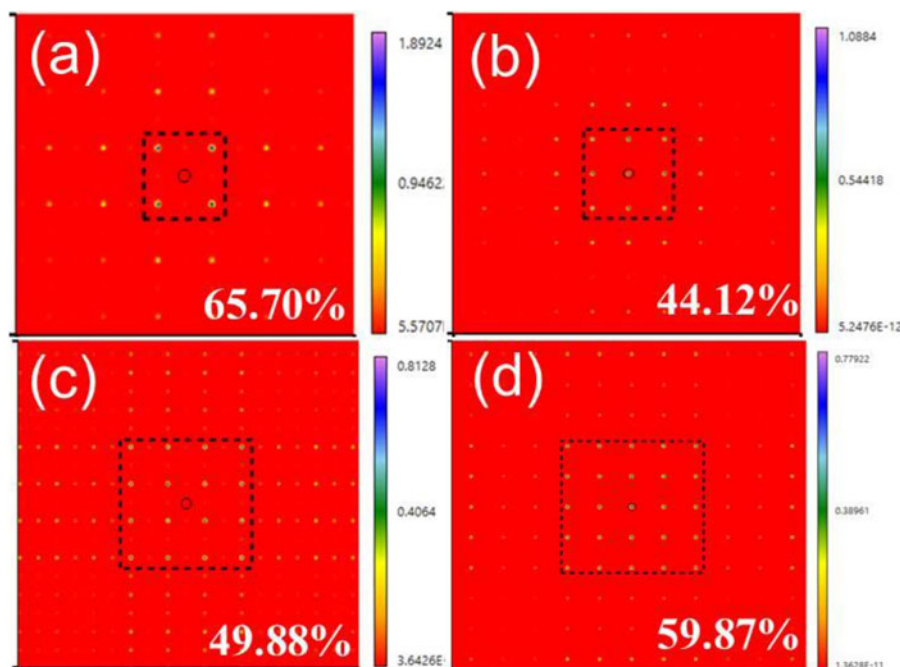


Fig. 5. Theoretical simulation of diffraction efficiency of DGs that generate (a) 2×2 , (b) 3×3 , (c) 4×4 , and (d) 5×5 spot sources are 65.70%, 44.12%, 49.88%, and 59.87%, respectively. The scale of color bar represents normalized intensity of amplitude.

laser induced refractive-index change in silica was estimated to be $\sim 10^{-3}$ [32]. The incident light has to travel much farther to reach π for phase shift in a material whose shift of the refractive index is rather small, which means a large thickness, whereby it always takes a long time to fabricate a Dammann grating in silica glass. Our processing method on sapphire surface have greatly reduced the machining time and thus improved the processing efficiency.

To observe the diffractive pattern of a DG, we adopted a continuous laser beam with the wavelength of 266 nm as the incident light. Fig. 4(a)–(d) shows the diffractive patterns of the DGs that each generates an array of 2×2 , 3×3 , 4×4 , and 5×5 spots, respectively. The diffractive efficiency of an odd-number-spot generator and of an even-number-spot generator is calculated by

$$\eta_{\text{odd}} = \left(I_0 + 2 \sum_{i=1}^N I_i \right) / I_{\text{inc}}. \quad (2)$$

$$\eta_{\text{even}} = \left(2 \sum_{i=1}^N I_{2i-1} \right) / I_{\text{inc}}. \quad (3)$$

Herein, η is the diffractive efficiency, I_0 is the intensity of the zero order, I_i is that of a higher order required in the fan-out, and I_{inc} is that of the incident light. Note that the zero order is not involved for an even number spot array generator. The diffractive efficiency of the gratings shown in Figs. 4(a)–4(d) was calculated to be 59.26%, 39.53%, 44.68%, and 55.37% in order. The difference between the predicted and experimental diffraction efficiency probably is due to the limited fabrication precision and wet etching tolerance and measurement error. Besides, they have slightly influence on the uniformity of the spot intensities, which is another criterion used to judge a Dammann grating. For an intuitional view, the uniformity is expressed as Fig. 4(e) and Fig. 4(f) show. Each peak indicates the intensity of its corresponding spot along the arrowed lines X and Y shown in Fig. 4(d); obviously, the uniformity of the spot intensities is excellent.

Energy distribution behind the DGs was simulated by commercial simulation software, VirtualLab grating toolbox trial version, which was based on the rigorous Fourier Modal Method. The far field fan-out pattern of intensity distribution of the spot array generated from the single layer grating with 3×3 periods is shown in Fig. 5, and the theoretical diffraction efficiency of DGs that generate 2×2 , 3×3 , 4×4 , 5×5 spot sources are 65.70%, 44.12%, 49.88%, and 59.87%, respectively. We have demonstrated the unique UV beam splitting capability in the experiment, showing a good agreement with simulation results.

4. Conclusion

In summary, DGs for UV beam splitting have been fabricated on sapphire by femtosecond laser writing and subsequent wet etching. Three key points are achieved in this work simultaneously. First, we report in this paper the first DGs working in ultraviolet region in contrast to the previously reported DGs (fabricated use photoresist, glass, silicon etc.) that working in visible region or infrared region. Second, excellent processing quality and optical performances for practical applications are achieved. Due to the excellent surface quality and 3-D geometry, the sapphire based DGs exhibited ideal and distinctive UV beam splitting properties, the diffraction efficiency of DGs that each generate 2×2 , 3×3 , 4×4 , and 5×5 spot sources is demonstrated to be 59.26%, 39.53%, 44.68%, and 55.37% respectively. Third, the uniformity of the spot intensities is excellent which means our DGs could create an array of spots with almost equal energy. Such sapphire-based DGs would have broad and distinctive application in UV beam shaping, UV beam splitting, and parallel laser processing.

Reference

- [1] H. Dammann and K. Görtler, "High-efficiency in-line multiple imaging by means of multiple phase holograms," *Opt. Commun.*, vol. 3, no. 5, pp. 312–315, Jul. 1971.
- [2] H. Dammann and E. Klotz, "Coherent optical generation and inspection of two-dimensional periodic structures," *J. Mod. Optic.*, vol. 24, no. 4, pp. 505–515, 1977.
- [3] J. N. Mait, "Design of Dammann gratings for two-dimensional, nonseparable, noncentrosymmetric responses," *Opt. Lett.*, vol. 14, no. 4, pp. 196–198, Feb. 1989.
- [4] S. Zhao and P. S. Chung, "Design of a circular Dammann grating," *Opt. Lett.*, vol. 31, no. 16, pp. 2387–2389, Aug. 2006.
- [5] B. Li *et al.*, "Design and sub-beam phase measurement of Dammann grating with three-phase array output," *Opt. Lett.*, vol. 38, no. 15, pp. 2663–2665, Aug. 2013.
- [6] C. H. Zhou and L. R. Liu "Numerical study of Dammann array illuminators," *Appl. Opt.*, vol. 34, no. 26, pp. 5961–5969, Sep. 1995.
- [7] Y. Li, W. Watanabe, T. Tamaki, J. Nishii, and K. Itoh, "Fabrication of Dammann gratings in silica glass using a filament of femtosecond laser," *Jpn. J. Appl. Phys.*, vol. 44, no. 7A, pp. 5014–5016, Jul. 2005.
- [8] U. Levy, B. Desiatov, I. Goykhman, T. Nachmias, A. Ohayon, and S. E. Meltzer, "Design, fabrication, and characterization of circular Dammann gratings based on grayscale lithography," *Opt. Lett.*, vol. 35, no. 6, pp. 880–882, Mar. 2010.
- [9] Q. D. Chen, X. F. Lin, L. G. Niu, D. Wu, W. Q. Wang, and H. B. Sun, "Dammann gratings as integratable micro-optical elements created by laser micromanofabrication via two-photon photopolymerization," *Opt. Lett.*, vol. 33, no. 21, pp. 2559–2561, Nov. 2008.
- [10] G. Li, C. Zhou, and E. Dai, "Splitting of femtosecond laser pulses by using a Dammann grating and compensation gratings," *J. Opt. Soc. Amer. A*, vol. 22, no. 4, pp. 767–772, Apr. 2005.
- [11] A. Yan, L. Liu, E. Dai, J. Sun, and Y. Zhou, "Simultaneous beam combination and aperture filling of coherent laser arrays by conjugate Dammann gratings," *Opt. Lett.*, vol. 35, no. 8, pp. 1251–1253, Apr. 2010.
- [12] Z. Kuang *et al.*, "Ultrafast laser parallel microprocessing using high uniformity binary Dammann grating generated beam array," *Appl. Surface Sci.*, vol. 273, pp. 101–106, Feb. 2013.
- [13] Y. Shinoda, J. P. Liu, P. S. Chung, K. Dobson, X. Zhou, and T. C. Poon, "Three-dimensional complex image coding using a circular Dammann grating," *Appl. Opt.*, vol. 50, no. 7, pp. B38–B45, Mar. 2011.
- [14] I. Moreno, J. A. Davis, D. M. Cottrell, N. Zhang, and X. C. Yuan, "Encoding generalized phase functions on Dammann gratings," *Opt. Lett.*, vol. 35, no. 10, pp. 1536–1538, May 2010.
- [15] J. A. Davis, I. Moreno, J. L. Martínez, T. J. Hernandez, and D. M. Cottrell, "Creating three-dimensional lattice patterns using programmable Dammann gratings," *Appl. Opt.*, vol. 50, no. 20, pp. 3653–3657, Jul. 2011.
- [16] J. J. Yu *et al.*, "Three-dimensional Dammann array," *Appl. Opt.*, vol. 51, no. 10, pp. 1619–1630, Apr. 2012.
- [17] N. Zhang, J. A. Davis, I. Moreno, D. M. Cottrell, and X. C. Yuan, "Analysis of multilevel spiral phase plates using a Dammann vortex sensing grating," *Opt. Exp.*, vol. 18, no. 25, pp. 25987–25992, Dec. 2010.
- [18] J. J. Yu, C. H. Zhou, W. Jia, A. D. Hu, S. Q. Wang, and J. Y. Ma, "Circular Dammann grating under high numerical aperture focusing," *Appl. Opt.*, vol. 51, no. 7, pp. 994–999, Mar. 2012.

- [19] Y. C. Zhang, N. Gao, and C. Q. Xie, "Using circular Dammann gratings to produce impulse optic vortex rings," *Appl. Phys. Lett.*, vol. 100, no. 4, Jan. 2012, Art. no. 041107.
- [20] J. J. Yu *et al.*, "Distorted Dammann grating," *Opt. Lett.*, vol. 38, no. 4, pp. 474–476, Feb. 2013.
- [21] T. Lei *et al.*, "Massive individual orbital angular momentum channels for multiplexing enabled by Dammann gratings," *Light Sci. Appl.*, vol. 4, no. 3, Mar. 2015, Art. no. e257.
- [22] N. Zhang, X. C. Yuan, and R. E. Burge, "Extending the detection range of optical vortices by Dammann vortex gratings," *Opt. Lett.*, vol. 35, no. 20, pp. 3495–3497, Oct. 2010.
- [23] Z. L. Li *et al.*, "All-silicon nanorod-based Dammann gratings," *Opt. Lett.*, vol. 40, no. 18, pp. 4285–4288, Sep. 2015.
- [24] C. M. Chang, M. H. Shiao, D. Chiang, C. T. Yang, M. J. Huang, and W. J. Hsueh, "Submicron-size patterning on the sapphire substrate prepared by nanosphere lithography and nanoimprint lithography techniques," *Metals Mater. Int.*, vol. 19, no. 4, pp. 869–874, Sep. 2013.
- [25] S. H. Lee, J. W. Leem, and J. S. Yu, "Transmittance enhancement of sapphires with antireflective subwavelength grating patterned UV polymer surface structures by soft lithography," *Opt. Exp.*, vol. 21, no. 24, pp. 29298–29303, Nov. 2013.
- [26] K. Sugioka and Y. Cheng, "Ultrafast lasers—Reliable tools for advanced materials processing," *Light Sci. Appl.*, vol. 3, Apr. 2014, Art. no. e149.
- [27] S. Juodkakis *et al.*, "Control over the crystalline state of sapphire," *Adv. Mater.*, vol. 18, no. 11, pp. 1361–1364, Apr. 2006.
- [28] R. Kammel *et al.*, "Enhancing precision in FS-laser material processing by simultaneous spatial and temporal focusing," *Light Sci. Appl.*, vol. 3, May 2014, Art. no. e169.
- [29] Q. K. Li *et al.*, "Sapphire-based Fresnel zone plate fabricated by femtosecond laser direct writing and wet etching," *IEEE Photon. Technol. Lett.*, vol. 28, no. 12, pp. 1290–1293, Jun. 2016.
- [30] T. Kudrius, G. Šlekys, and S. Juodkakis, "Surface-texturing of sapphire by femtosecond laser pulses for photonic applications," *J. Phys. D, Appl. Phys.*, vol. 43, no. 14, pp. 145501–145505, Mar. 2010.
- [31] Y. D. Li, W. Watanabe, T. Tamaki, J. Nishii, and K. Itoh, "Fabrication of Dammann gratings in silica glass using a filament of femtosecond laser," *Jpn. J. Appl. Phys.*, vol. 44, no. 7A, pp. 5014–5016, Jul. 2005.
- [32] K. Yamada, W. Watanabe, Y. D. Li, K. Itoh, and J. Nishii, "Multilevel phase-type diffractive lenses in silica glass induced by filamentation of femtosecond laser pulses," *Opt. Lett.*, vol. 29, no. 16, pp. 1846–1848, Aug. 2004.